

# Two-Dimensional Molecular Electronics Circuits

Yi Luo, C. Patrick Collier, Jan O. Jeppesen, Kent A. Nielsen, Erica Delonno, Greg Ho, Julie Perkins, Hsian-Rong Tseng, Tohru Yamamoto, J. Fraser Stoddart,\* and James R. Heath\*[a]

Addressing an array of bistable [2]rotaxanes through a two-dimensional crossbar arrangement provides the device element of a current-driven molecular electronic circuit. The development of the [2]rotaxane switches through an iterative, evolutionary process

is described. The arrangement reported here allows both memory and logic functions to use the same elements.

## KEYWORDS:

amphiphilic bistable [2]rotaxanes · crossbars · logic · memory · molecular devices · molecular electronics

One of the most exciting developments in science and engineering over the past few years has been the progress toward architectures,<sup>[1]</sup> materials,<sup>[2]</sup> and devices<sup>[3]</sup> for nanoscale and molecular-electronics-based computing systems. Metrics for progress in this field include the advancing capabilities of the devices themselves, as well as the movement toward increasingly complex arrangements of devices and circuits. One way to categorize these advances is through their architectural complexity. In Figure 1 we present a pathway toward increasingly complex circuits, starting with isolated devices and ending with a two-dimensional (2D) crossbar circuit that has been configured for logic applications. While the crossbar is not the only 2D circuit architecture that is being explored for nanoelectronics, it

is the dominant one for a variety of reasons, which include the following: a) A crossbar tiles in 2D and involves only two sets of straight, aligned wires. Thus, crossbars may be fabricated using a wide variety of techniques, ranging from traditional lithography to imprinting and the chemical assembly of nanowires.<sup>[4–6]</sup> b) Since a crossbar may be addressed using order ( $n$ ) number of large wires to interrogate  $2^n$  nanowires, it can exhibit excellent scaling between the micro and nano length scales.<sup>[7]</sup> c) The crossbar is a generic circuit that can be electronically configured for memory, logic, or signal routing applications without the requirement of gain, although signal gain is, of course, an eventual requirement. d) Nanoelectronic circuits that involve some level of chemical assembly in the fabrication process are unlikely to be perfect, and the crossbar structure is defect-tolerant. Note that, for the 2D logic circuit, two entire rows of devices are not utilized, and those rows could represent defective components. e) For very high device densities, power consumption may outweigh other metrics, such as switching speed. A crossbar can be a naturally parallel architecture and so switching speed is not a particularly important metric. For a crossbar-based memory in which each junction represents a memory bit, up to 50% of the memory bits may be written at the speed of a single device. In Figure 1 (in the second row of the 2D Memory Circuit) we illustrate how, for example, a row of memory bits might be written in parallel to store the number “0101”. Thus, the speed of a crossbar circuit is limited by the size of the crossbar and by how the crossbar is addressed, but not by the speed of a single device within the crossbar.

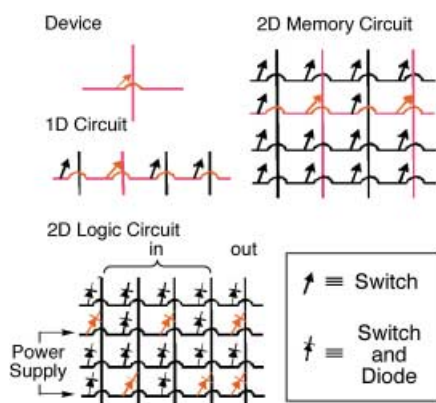


**Figure 1.** A simple yet versatile circuit architecture, known as a crossbar, is shown at increasing levels of complexity in terms of both fabrication and function. Each junction is a switching device, with black arrows corresponding to open switches and red arrows to closed switches. Wires that are utilized to address or modify the switches are highlighted in red, except for the case of the 2D Logic Circuit in which the configuration of the circuit (where the junctions are both switches and diodes) has been indicated. In the 1D circuit, the number “0100” is stored by addressing the second device (crossbar highlighted in red) and closing the switch. In the 2D Memory Circuit, the number “0101” is stored by writing the second row (red) with the second and fourth columns (red) in parallel. In the 2D Logic Circuit, the switches are configured in such a way that six of them are closed (red) so that the circuit can perform as a half-adder.

[a] Prof. J. F. Stoddart, Prof. J. R. Heath, Dr. Y. Luo, Dr. C. P. Collier, Dr. J. O. Jeppesen, K. A. Nielsen, E. Delonno, G. Ho, Dr. J. Perkins, Dr. H.-R. Tseng, T. Yamamoto  
The California NanoSystems Institute  
and Department of Chemistry and Biochemistry  
University of California, Los Angeles  
603 Charles E. Young East Drive, Los Angeles, CA 90095-1569 (USA)  
Fax: (+1) 310-206-4038  
E-mail: stoddart@chem.ucla.edu, heath@chem.ucla.edu

Supporting information for this article is available on the WWW under <http://www.chemphyschem.com> or from the author.

Each junction in a crossbar represents an active device that may be fabricated through the crossing of, for example, just two wires, possibly separated by some insulating dielectric, or two wires sandwiching some active molecular component. Bistable nanotube mechanical junctions,<sup>[8]</sup> as well as various molecular sandwich junction devices—diodes,<sup>[9]</sup> molecular switch tunnel junctions,<sup>[10]</sup> and junctions exhibiting negative differential resistance<sup>[11]</sup>—have all been demonstrated at the device level.

The one-dimensional (1D) circuit represents an additional level in complexity and is the current state-of-the-art. Once again, there are multiple ways of fabricating and utilizing such a structure. In one variation, it can represent a series of (nanowire) transistors; these are three-terminal devices in which the active switching components are the wires. By using the vertical wires as gates for nanowire field-effect transistors (FETs), both Dekker's<sup>[12]</sup> and Lieber's<sup>[13]</sup> groups have demonstrated gain elements and fundamental logic gates exhibiting, for example, AND and NOR functions. A second possibility for 1D circuits would be a series of two-terminal tunnel junctions containing a molecular component in which the wires are passive conductors and the molecular component is the active switching element. Although such circuits cannot provide signal gain, singly configurable molecular switch tunnel junctions have been demonstrated as wired-logic (AND and OR) functions using this architecture.<sup>[14]</sup>

The transition from 1D to 2D crossbar circuits represents a significant step forward in complexity and places serious constraints on the types of devices that can be utilized within the circuit. While examples of potentially scalable fabrication approaches for the chemical assembly of nanowire crossbars have appeared in the recent literature,<sup>[15, 16]</sup> it is not obvious that nanowire three-terminal devices (transistors) can be used in a 2D crossbar. Consider, for example, a 1D circuit made of nanowire-based FETs in which the vertically oriented wires are gates. For that circuit, the horizontal wire serves as an alternating series of source and drain junctions for each gate, and the signal through that wire is modulated by the gates. If the 1D circuit is extended into a 2D crossbar, then the application of a gate voltage onto just one of the vertical wires will affect all horizontal signal-carrying wires equally. The fundamental issue here is that a 2D crossbar is fully utilized only if each junction, or point, is individually and separately addressable. The Teramac computer,<sup>[17]</sup> from which the defect-tolerant crossbar architecture for nanoelectronics circuitry was extracted, did utilize a transistor-based crossbar. However, each "point" in the crossbar was itself a small circuit consisting of six transistors.<sup>[1]</sup> While a more natural tiling of three-terminal devices would be a hexagonal grid, such a geometry is intrinsically not point-addressable.<sup>[3]</sup>

Two terminal switching devices are, however, attractive candidates for 2D crossbar circuitry and, in fact, crossbar-based random access memories have been investigated for many

years. Most work has focused on ferroelectric<sup>[17]</sup> and magneto-resistive<sup>[18]</sup> crosspoint memories—FeRAM and MagRAM, respectively. The electrical resistance of these junctions exhibits a hysteretic response to an applied field and so they may serve as the basis for nonvolatile information storage. However, these systems also exhibit significant problems with respect to point addressability. While neither FeRAM nor MagRAM are likely to scale to true nanoscale dimensions, it is instructive to consider them as examples in light of what is important to get a crosspoint memory to work. Consider how the 2D memory circuit is addressed in Figure 1. For MagRAM or FeRAM, a field is used to "pole" a given device. Poling may be done by applying a voltage  $V_A$  across the two wires that define that junction. In practice,  $V_A$  is split into two components,  $-\frac{1}{2}V_A$  and  $+\frac{1}{2}V_A$ , which are then applied to the top and bottom wires. Thus, all the junctions in a given row or column are subjected to at least half the applied field. In fact, in a crossbar circuit, all of the devices are electrically interconnected, and so every junction in the circuit is subjected to at least some field. In field-poled junctions, the field generated by  $\pm\frac{1}{2}V_A$  is occasionally sufficient to alter the state of a device since the poling process itself is based on a field-driven nucleation event. Nucleation events in general are subject to statistical fluctuations, and the poling of FeRAM or MagRAM bits is no exception. The problem of accidentally setting a bit is known as the " $-\frac{1}{2}$  voltage select" or the "half-select" problem. This problem has seriously limited the development of crossbar memories and is likely a generic problem for field-poled devices. Configuring a 2D crossbar for logic (see the 2D Logic Circuit in Figure 1) places significant further constraints on the junction requirements. We will return to this issue at the end of this Article.

We have reported<sup>[10]</sup> previously on molecular switch tunnel junctions (MSTJs) that are two-terminal devices, similar to the FeRAM or MagRAM junctions. They exhibit a hysteretic response to an applied voltage (not field) and so can also serve as the basis for information storage. However, the actual mechanism by which MSTJs are switched is unique (Figure 2). The first switches that we reported were based on molecular mechanical motion that was activated in a bistable [2]catenane (Figure 3a) by current flowing through particular molecular electronic states. This means that, if the Fermi levels of the electrodes were not lined up with the appropriate electronic states of the molecules in the junctions, then the molecules did not switch. Our MSTJs are not field-activated switches. Instead, they are single-molecule-thick electrochemical cells that are characterized by signature voltages at which current flows and the molecules switch. Because the switching is a molecular property, the switching process itself is not characterized by nucleation statistics. Thus, MSTJs are promising candidates for the active elements of 2D Memory Circuits (Figure 1), since they have the potential to avoid the half-select problem. Furthermore, if the switching response is based on a molecular signature, then these devices should scale to nanometer dimensions without significant changes in performance.

In this Article, we present the outcome of an evolutionary process in molecular design and synthesis involving a progression from the bistable [2]catenane, via a bistable [2]pseudo-

[\*] Hewlett-Packard's Teramac, a prototype for a custom-configurable computer, uses multiply redundant and highly interconnected chips; like the Internet, the Teramac is defect-tolerant and routes around flaws. Another design departure is in the Teramac's logical operations, which are conducted in memory chips storing the answers to logical operations in look-up tables

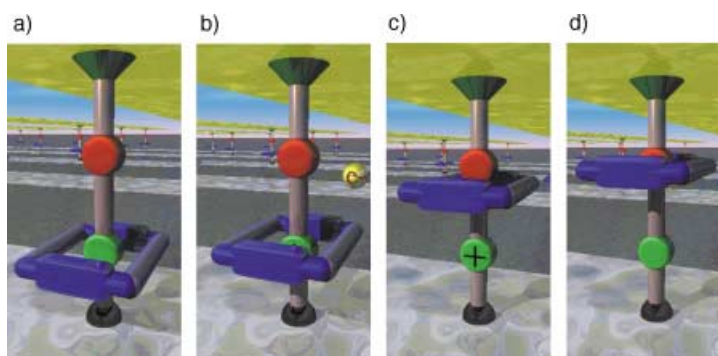


**Figure 2.** A graphical representation of a molecular switch tunnel junction based on a bistable [2]rotaxane. This molecule consists of 1) an amphiphilic dumbbell component containing two recognition sites: a tetrathiafulvalene (TTF) unit (green) and a dioxynaphthalene (DNP) ring system (red), and two stoppers, one (upper) hydrophobic (dark green), the other (lower) hydrophilic (black), and 2) a ring component, the tetracationic cyclophane (blue), cyclobis(paraquat-p-phenylene). a) In the beginning, the positively charged ring encircles the TTF recognition site on the dumbbell component. b) Oxidation of the TTF unit converts it to a radical cation ( $\text{TTF}^+$ ) which leads to Coulombic repulsion of the tetracationic cyclophane and c) its translation up to the neutral DNP site. d) Finally, the  $\text{TTF}^+$  is reduced, leaving the bistable [2]rotaxane in a metastable state. These two mechanically distinguishable states, shown in (a) and (d), exhibit different characteristic tunneling currents. Since the mechanical motion is an activated process, these devices exhibit a hysteretic current–voltage response. The activation process that leads to the reinstatement of the stable state (a) of the switch from its metastable state (d) could be thermally and/or voltage driven by, for example, reduction of the bipyridinium units in the cyclophane to radical cations.

rotaxane, to a pair of amphiphilic, bistable [2]rotaxanes. This process was driven by feedback from solid-state MSTJ device performance, and driven by the requirements of achieving point

addressability and large-amplitude switching within a 2D crossbar circuit. We demonstrate that the device characteristics are retained as micrometer-scale MSTJs containing  $10^7$  molecules are scaled down to nanometer-scale MSTJs that contain just a few thousand molecules. We then demonstrate point addressability of MSTJs through the operation of a 64-bit 2D crossbar random access memory circuit. Next, we return to the 2D crossbar circuit for logic applications. We discuss the additional requirements of that circuit, followed by a demonstration of what is currently possible—a circuit of two coupled, complementary 1D logic gates to achieve an XOR function. Finally, we discuss the challenges that lie ahead for configuring an entire finite-state computing machine from molecular-switch based 2D crossbars.

We have reported<sup>[10]</sup> previously on resettable MSTJ devices based on a bistable [2]catenane (Figure 3 a). These devices exhibited roughly a factor of 100% ( $= \times 2$ ) change in junction resistance between the “0” and “1” states, and could be cycled, under ambient conditions, at least a few hundred times. More importantly, the voltages required to open or close the switches were stable from one switching cycle to the next and from device to device. Various control devices, including those containing degenerate, monostable [2]catenanes,<sup>[19]</sup> demonstrated that bistability in the [2]catenane structure was critical for switching. The MSTJ switching was thermally activated, consistent with a mechanism involving molecular motion. These and other results<sup>[20]</sup> imply that at least some critical aspect of the

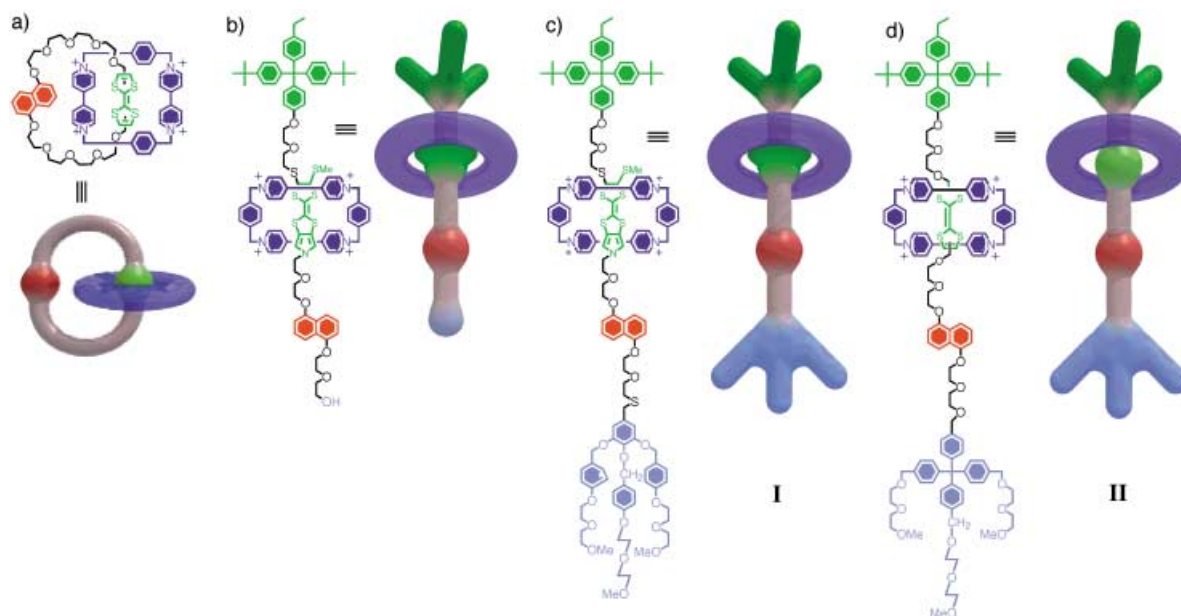


**Figure 3.** From left to right, (supra)molecular structures and graphical representations of the mechanically interlocked (complex) evolved empirically according to the device requirements for achieving point addressability and high amplitude switching within a 2D crossbar circuit. a) A bistable [2]catenane. b) An amphiphilic, bistable [2]pseudorotaxane. c, d) The I and II versions, respectively, of amphiphilic, bistable [2]rotaxanes. In all of these mechanical switches, the solution-phase switching mechanism is based on oxidation of the tetrathiafulvalene (TTF) unit (green), followed by Coulombic repulsion-driven motion of the tetracationic cyclophane component (blue) so that it encircles the dioxynaphthalene (DNP) ring system (red). Note that, while the starting states of the [2]catenane and [2]rotaxane II, shown in (a) and (d) respectively, exist as one co-conformation (where the blue ring encircles only the green site) in solution, the [2]pseudorotaxane and the [2]rotaxane I, shown in (b) and (c) respectively, exist as approximately 1:1 mixtures of both co-conformations (where the green and red sites are encircled more or less equally by the blue ring). This observation might imply that, in solid-state devices, only half of these (supra)molecules would, at most, be active switches.

solution-phase electrochemical switching mechanism<sup>[21]</sup> was retained in the solid-state device. However, the [2]catenane devices exhibited two problems that limited their usefulness in 2D crossbar circuits. First, the current levels through the [2]catenane MSTJs were low, with only about 20 pA (at 0.1 V) recorded in the switch-closed state. Second, while the switching magnitude was larger than is observed for MagRAM or FeRAM devices, it was not sufficient for use in a 2D crossbar logic circuit.

For the [2]catenane-based MSTJs, the actual electrochemically active component of the molecule—the [2]catenane itself—was located near the polysilicon electrode whereas long-chain phospholipid counterions—used to make the compound amphiphilic—bridge the bulk of the gap between the two electrodes. The [2]pseudorotaxane (Figure 3b) was designed as a way of placing the redox-active components more symmetrically between the electrodes in order to increase the resonant tunneling current. This switch did, in fact, exhibit much higher current levels (100 nA at 0.1 V) in the switch-closed state and the change in junction resistance upon switching approached a factor of 10000%. However, these MSTJs exhibited large current amplitude fluctuations in the cycling between the closed and open states, and the voltages required to address the switches were poorly defined.<sup>[3]</sup> This is exactly the type of signature that renders a MSTJ useless within a 2D crossbar circuit. Various optical and scanning probe measurements of the [2]pseudorotaxane films revealed<sup>[20]</sup> the presence of molecular domains that were 1  $\mu\text{m}$  in diameter or larger. The presence of these domains, coupled with the erratic device characteristics, indicated that the molecular components were not acting individually but rather as domains, and that domain switching was most likely dominating device performance. Domain switching bears similarities to the MagRAM and FeRAM mechanisms in that it is a phenomenon driven by nucleation statistics. Our conclusion was that there was not sufficient area per molecule to allow for individual molecular reorganization unless the entire domain reorganized at the same time. Because of the poorly defined address voltages, the [2]pseudorotaxane devices, while operable as switches, were not useful as components of a 2D crossbar.

Next, we devised a synthetic strategy to avoid domain switching while still retaining a molecular architecture similar to that of the [2]pseudorotaxane. This strategy is embodied in the amphiphilic, bistable [2]rotaxane I shown in Figure 3c. This molecule has a much larger footprint in a monolayer film (140  $\text{\AA}^2$ , as compared to about 40  $\text{\AA}^2$  for the [2]pseudorotaxane) as a result of incorporating a dendron as the hydrophilic stopper in the dumbbell component. Thus, there is simply more area per molecule to accommodate the molecular reorganizations. No domains were detected with either Brewster angle microscopy or with various scanning probe microscopy techniques.

In the final iteration of the structure–performance relationship between device performance and molecular structure, the amphiphilic, bistable [2]rotaxane I was replaced by the variant II (Figure 3d). The reasons for this change were a) to produce a molecular switch in which the amphiphilic, bistable [2]rotaxane starts off exclusively as only one of its two possible conformations and b) to invest in that switch enhanced

oxidative stability by removing all the phenolic residues from the hydrophilic stopper.

For all devices, the molecules were self-organized as Langmuir monolayers before being transferred to a substrate patterned with n-type polysilicon electrodes. Devices and circuits containing MSTJ junctions, defined by micrometer-scale patterning through a combination of optical lithography and (top) electrode deposition through shadow masks, were fabricated as previously described.<sup>[14, 20]</sup> However, the ability of these MSTJs to retain their operational characteristics at much smaller device dimensions is critical to the central arguments of this paper. Thus, we developed a scalable fabrication process for making 2D crossbars containing nanometer scale MSTJs. This process is described here for the first time. Isolated, nanometer-scale molecular devices can be demonstrated, for example, using break junctions,<sup>[22]</sup> nanopore structures,<sup>[11]</sup> or scanning probe techniques.<sup>[23]</sup> However, those methods are not practical for more than a few devices. Furthermore, the shadow mask approaches utilized for defining the micrometer scale junctions do not scale easily to junction dimensions of even one square micrometer. Thus, size-sealing even a simple circuit like a 2D molecular switch crossbar requires that the patterning itself be carried out directly on top of the molecular monolayer. We have developed such a process by utilizing the titanium adhesion layer as a protective coat of the molecular LB monolayer upon which photo- or electron-beam resists can be deposited, patterned, and developed, as described in the Supporting Information.<sup>[25]</sup> This technique was utilized to demonstrate device scaling (Figure 4) to junction areas of 0.005 to 0.01  $\mu\text{m}^2$ . These devices behaved very similarly to the micrometer-scale devices, albeit with reduced current levels.

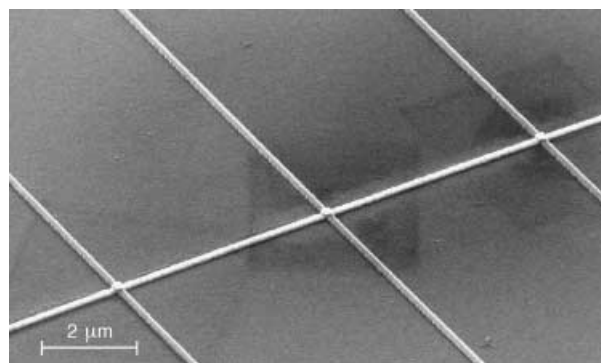


**Figure 4.** A SEM image of a 1D circuit of MSTJs (scale bar 2  $\mu\text{m}$ ). Each junction has an area of 0.007  $\mu\text{m}^2$  and contains about 5000 molecules. The inter-wire separation distance was kept large so as to simplify the task of contacting this circuit to external devices for testing.

For all devices, a top electrode (5–15 nm of titanium followed by 100 nm of aluminum or aluminum plus nickel) was deposited by electron-beam evaporation. For single device measurements, bias voltages were applied to the polysilicon electrode, while the top electrode was grounded through a current preamplifier. For the 2D crossbar circuit measurements, a relay switching matrix was utilized to achieve independent control over every wire. Junctions were opened or closed by splitting the address

voltage across the top and bottom wires that defined the junction, while all other wires were held at ground. After some string of bits was configured into the memory, the entire memory was read out by applying a small voltage (between  $-0.2$  and  $+0.2$  V) to the top wire and grounding the bottom wire through a current preamplifier while, again, all other wires were held at ground.

MSTJs based on the amphiphilic, bistable [2]rotaxanes I and II exhibited similar device signatures<sup>[24]</sup> to each other, and those signatures did not change as the devices were scaled from the micrometer- to the nanometer-scale junctions (Figure 5). A switch-closed current level of approximately 1 nA (at 0.1 V) was observed in the larger devices, and, for both sizes of devices, the closed/open switching amplitude varied from 300% to 1000%. Most importantly, however, was the fact that the voltages required to open and close the MSTJs in I and II had characteristic and stable values at around  $-2$  and  $+2$  V, respectively. Moreover, these values did not change as the devices were repeatedly cycled between the closed and open states. Several

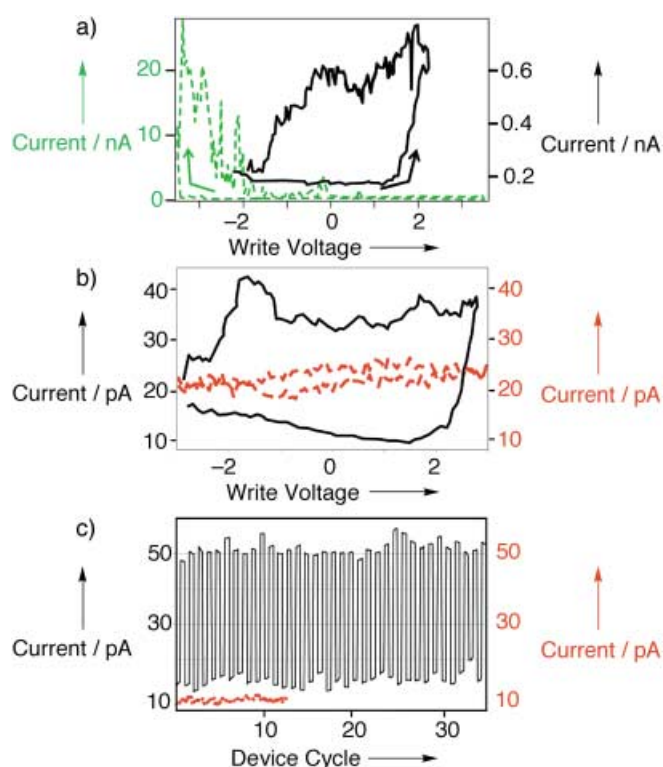


**Figure 5.** Device characteristics (solid black lines) of a) micrometer- and b, c) nanometer-scale MSTJs, all based on a bistable [2] rotaxane I monolayer sandwiched between two electrodes. Also shown are the responses of control molecules—the dumbbell component of the [2]rotaxane (green dashed trace in (a) and eicosanoic acid ( $C_{19}H_{39}CO_2H$ ) (red dashed traces in (b) and (c)). Traces (a) and (b) correspond to measurements of the remnant molecular signature hysteresis loop, which is obtained by reading, at low voltage, the response of the junction to a series of voltage pulses that map out the hysteresis loop. This loop defines the voltages for opening ( $\approx +2$  V) and closing ( $\approx -2$  V) the switches. The black trace in (c) represents 35 cycles of the nanometer-scale device, recorded by repeatedly closing and opening the switch, and then monitoring the current through the junction, at 0.1 V applied bias, after each writing event. The dumbbell control device exhibits electrical breakdown near  $-3.5$  V, but otherwise both it and the eicosanoic acid junctions act as simple tunnel barriers (see the red traces in (b) and (c)).

control devices were fabricated, including devices that utilized the dumbbell component (everything but the ring) of the [2]rotaxane I (Figure 5 a) and eicosanoic acid (Figures 5 b and 5 c). These controls indicated that a fully assembled, bistable [2]rotaxane was critical for achieving the switching response.<sup>[20, 25]</sup> In the case of the dumbbell component controls, no switching response was observed up to biases of  $\pm 3$  V, above which a sharp current jump that we attribute to electrical breakdown was recorded (Figure 5 a). Such a breakdown, which is expected at high fields, has been observed in virtually every molecular junction that we have investigated. In all other aspects, the control devices simply acted as passive tunnel barriers. The switching response of the [2]rotaxane-based MSTJs were dramatically improved if very strict attention was paid during the device fabrication to chemical properties such as the pH of the subphase and of the chloroform spreading solvent—both of which must be kept slightly basic so as to prevent degradation of the tetrathiafulvalene units.<sup>[26]</sup> In common with the case for the [2]catenane-based MSTJs, the switching mechanism in the [2]rotaxane-based MSTJs was thermally activated, and all switching was quenched at 260 K. The switch-open state is stable over arbitrarily long periods of time, while the switch-closed state relaxes to the switch-open state with an inverse exponential decay time of about 10–15 min.

A lesson we have learned from these investigations is that it is possible, by feeding device performance characteristics back into molecular synthesis, to improve the switching characteristics of a device. This feedback cycle would be tremendously aided by having a common analytical technique, such as some optical spectroscopy, that could interrogate the switching mechanism in the solution phase, in the molecular monolayer film, and, most critically, within the solid-state device. As it is, the mechanistic arguments, such as those portrayed in Figure 2, are phenomenologically based. They are extracted from the known solution-phase mechanisms but are not directly measured in the solid-state devices. Nevertheless, as described below, the [2]rotaxane-based MSTJs did work within the demanding constraints of a 2D crossbar circuit. We are encouraged that this molecular device was arrived at by a rational sequence of design and synthesis that was driven by chemical intuition and device performance.

The ultimate test of these switching devices is whether or not they exhibit point addressability within 2D crossbar circuits. Such circuits were fabricated from both micrometer- and nanometer-scale MSTJs. For the nanometer-scale devices, the yield of working junctions within a 2D crossbar circuit was only about 15–25%. This low yield for the small devices was attributable to broken wires in the circuit, a feature which is a byproduct of fabrication cleanliness. During the device fabrication process, the fact that the wafers were transported multiple times between the chemistry laboratory and two different fabrication facilities undoubtedly affected device yield. Although all junctions for which the wires were intact yielded operable devices, the low yield precluded a convincing demonstration of point addressability. For the larger (micrometer-scale) junctions using [2]rotaxane II, and where the yield of useable bits was substantially higher (80–100%), we were able to investigate

the issues of point addressability in 64-junction, 2D MSTJ crossbars. We accomplished this goal by utilizing the circuits as 64-bit random access memories, and then storing certain character strings, using the standard ASCII character set, into the memories. Once the character strings were stored in the memory, the entire memory was then read out. In Figure 6, we present the results of such testing. This and other similar circuits were cycled as memories several times and half-select problems were never encountered.

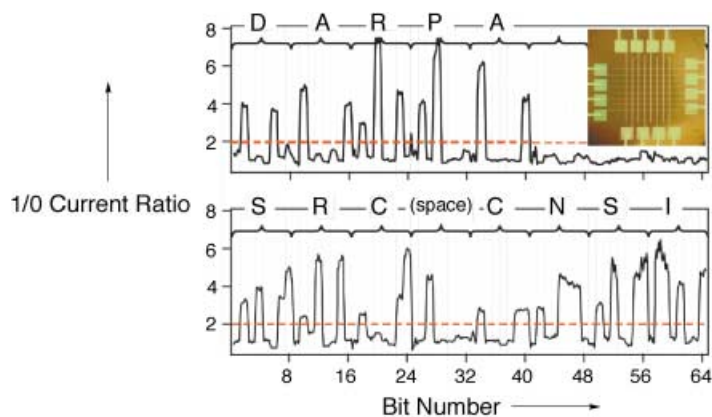


**Figure 6.** The demonstration of point addressability within a 64-bit molecular switch crossbar circuit (inset), utilized as a random access memory. This device was fabricated using the amphiphilic, bistable [2]rotaxane II. The use of the 64-bit molecular switch crossbar circuit to store the words DARPA (Defense Advanced Research Agency), SRC (Semiconductor Research Corporation), and CNSI (California NanoSystems Institute) is demonstrated. A character string of 1s and 0s, that corresponded to the standard ASCII characters for the indicated alphanumeric symbols, was stored and then the entire memory was sequentially read out. For example, an “R” character (ASCII 82), used in both the top and bottom character strings, is stored as the eight-bit number “01010010”. The red dashed line indicates the separation between 1s and 0s.

Finally we return to Figure 1—the 2D Logic Circuit. In this Figure, we have shown how this circuit may be utilized for wired-logic applications. Simple circuits using complementary logic, such as half-adders, may be configured by selectively opening and closing certain switches in the crossbar. The requirements of the individual junctions here are substantially more stringent than are needed for the memory circuit. The circuit must not only exhibit point addressability, but the junctions must be diodes as well as switches. Furthermore, the amplitude of the switching effect must be relatively large, since the output of the circuit is the result of routing an input through two or more junctions, each of which will dissipate the input signal level. MagRAM and FeRAM junctions typically exhibit 15% to 30% changes in junction resistance when the junction is poled, and so they simply cannot be used for logic applications. The MSTJs presented above are characterized by switching amplitudes that are at least an order of magnitude larger than for the ferroelectric or magnetoresistive analogues. Thus, our 2D MSTJ crossbars lack only the diode character necessary for logic applications. However, by selectively hard-wiring 1D circuits, the performance of a 2D logic crossbar containing diodes can be experimentally approximated. We present the results from such

a measurement, carried out using the version II [2]rotaxane-based MSTJs, in Figure 7. Here, we have generated an XOR function from two 1D circuits. This result, taken together with our previously published<sup>[14]</sup> (and simpler) AND gate, indicates that a simple half-adder function may be configured from a 2D MSTJ crossbar circuit if an appropriate diode response can be built into the junctions. We note that, while this approach of wired, complementary configurable logic is probably not a great way of doing logic, for limited applications and in potentially defective circuits it may work just fine.

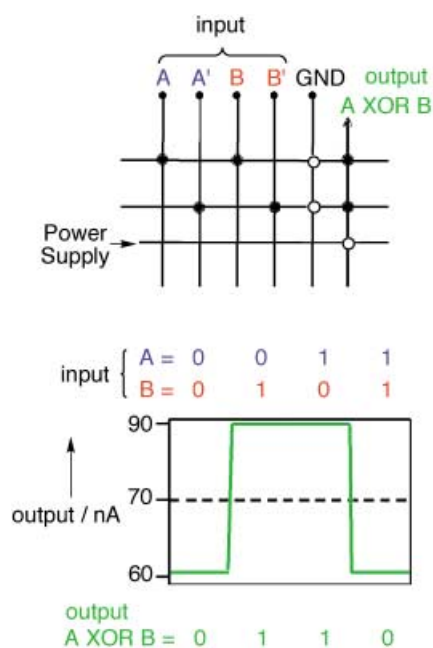


**Figure 7.** a) The wiring diagram and b) experimentally derived truth table of an XOR gate. In the wiring diagram, ● represent closed switches and ○ represent open switches. The junctions that are not dotted, which would be diodes in an ideal molecular-switch crossbar circuit, are not connected. A' and B' are the complements of A and B. An AND (which is a simpler structure) and an XOR function combine to yield a half-adder, with the XOR representing the sum of two 1-bit numbers and the AND representing the carry. In the experimentally derived truth table, the green trace is the output signal recorded corresponding to four different input combinations.

Finally, in order to couple the output of a true 2D MSTJ crossbar logic circuit with an MSTJ-based random access memory, signal gain<sup>[27]</sup> coupled with a clocking scheme will be required. If such a challenge can be met, then a simple demonstration of a molecular-electronics based finite-state computing machine—namely a machine that involves logic and memory talking to each other and to the outside world—should be possible.<sup>[27]</sup>

This work was supported primarily by the Defense Advanced Research Projects Agency (DARPA) with partial support from the Semiconductor Research Corporation (SRC). Some of the molecular characterization work was supported by the National Science Foundation. C.P.C. was an employee of the Hewlett–Packard Corporation. J.O.J. thanks the University of Odense for a PhD

Scholarship. T.Y. thanks Showa Denko K K for a Visiting Scholar Fellowship. We would like to acknowledge assistance from the UCLA Nanolab and the UCSB fabrication facility.

- [1] J. R. Heath, P. J. Kuekes, G. S. Snider, R. S. Williams, *Science* **1998**, *280*, 1716–1721.
- [2] A. M. Morales, C. M. Lieber, *Science* **1998**, *279*, 208–211.
- [3] A. R. Pease, J. O. Jeppesen, J. F. Stoddart, Y. Luo, C. P. Collier, J. R. Heath, *Acc. Chem. Res.* **2001**, *34*, 433–444.
- [4] B. Messer, J. H. Song, P. Yang, *J. Am. Chem. Soc.* **2000**, *122*, 10232–10233.
- [5] Y. Zhang, A. Chang, J. Cao, Q. Wang, W. Kim, Y. Li, N. Morris, E. Yenilmez, J. Kong, H. Dai, *Appl. Phys. Lett.* **2001**, *79*, 3155–3157.
- [6] B. R. Martin, D. C. Furnange, T. N. Jackson, T. E. Mallouk, T. S. Mayer, *Adv. Funct. Mater.* **2001**, *11*, 381–386.
- [7] “Demultiplexer for a Molecular Wire Crossbar Network”: P. J. Kuekes, R. S. Williams, *US Patent 6256767*, **2001**.
- [8] T. Rueckes, K. Kim, E. Joselevich, G. Y. Tseng, C.-L. Cheung, C. M. Lieber, *Science* **2000**, *289*, 94–97.
- [9] R. M. Metzger, *Acc. Chem. Res.* **1999**, *32*, 950–957.
- [10] C. P. Collier, G. Mattersteig, E. W. Wong, Y. Luo, K. Beverly, J. Sampaio, F. M. Raymo, J. F. Stoddart, J. R. Heath, *Science* **2000**, *289*, 1172–1175.
- [11] M. A. Reed, J. M. Tour, *Sci. Am.* **2000**, *282*, 86–93.
- [12] A. Bachtold, P. Hadley, T. Nakanishi, C. Dekker, *Science* **2001**, *294*, 1317–1320.
- [13] Y. Huang, X. Duan, Y. Cui, L. J. Lauhon, K.-H. Kim, C. M. Lieber, *Science* **2001**, *294*, 1313–1317.
- [14] C. P. Collier, E. W. Wong, M. Belohradsky, F. M. Raymo, J. F. Stoddart, P. J. Kuekes, R. S. Williams, J. R. Heath, *Science* **1999**, *285*, 391–394.
- [15] Y. Huang, X. Duan, Q. Wei, C. M. Lieber, *Science* **2001**, *291*, 630–633.
- [16] M. R. Diehl, S. N. Yaliraki, R. A. Beckman, M. Barahona, J. R. Heath, *Angew. Chem.* **2002**, *114*, 363–366; *Angew. Chem. Int. Ed.* **2002**, *41*, 353–356.
- [17] R. E. Jones, Jr., P. D. Maniar, R. Moazzami, P. Zurcher, J. Z. Witowski, Y. T. Lii, P. Chu, S. J. Gillespie, *Thin Solid Films* **1995**, *270*, 584–588.
- [18] S. S. P. Parkin, K. P. Roche, M. G. Samant, P. M. Rice, R. B. Beyers, R. E. Scheuerlein, E. J. O’Sullivan, S. L. Brown, J. Bucchigano, D. W. Abraham, Y. Lu, M. Rooks, P. L. Trouilloud, R. A. Wanner, W. J. Gallagher, *J. Appl. Phys.* **1999**, *85*, 5828–5833.
- [19] C. L. Brown, U. Jonas, J. A. Preece, H. Ringsdorf, M. Seitz, J. F. Stoddart, *Langmuir* **2000**, *16*, 1924–1930.
- [20] C. P. Collier, J. O. Jeppesen, Y. Luo, J. Perkins, E. W. Wong, J. R. Heath, J. F. Stoddart, *J. Am. Chem. Soc.* **2001**, *123*, 12632–12641.
- [21] V. Balzani, A. Credi, G. Mattersteig, O. A. Matthews, F. M. Raymo, J. F. Stoddart, M. S. Venturi, A. J. P. White, D. J. Williams, *J. Org. Chem.* **2000**, *65*, 1924–1936.
- [22] H. Park, J. Park, A. K. L. Lim, E. H. Anderson, A. P. Alivisatos, P. L. McEuen, *Nature* **2000**, *407*, 57–60.
- [23] Y. Xue, S. Datta, S. Hong, R. Reifenberger, J. I. Henderson, C. P. Kubiak, *Phys. Rev. B* **1999**, *59*, R7852–R7855.
- [24] MSTJs based on version II of the amphiphilic, bistable [2]rotaxane performed with a slightly increased switching amplitude over similar junctions that utilized version I. In addition, for 2D Memory Circuits, that employed MSTJs fabricated from the [2]rotaxane II, a higher yield of operable junctions was obtained. Whether or not this higher yield was related to the enhanced stability of the hydrophilic stopper (without any phenolic residues) in the [2]rotaxane II is not clear.
- [25] This material describes a) the synthesis of the key compounds used in this investigation, b) the device characteristics of a number of control devices that were fabricated from components of the mechanically interlocked molecules which behave as molecular switches, and c) certain processing techniques employed in the device fabrication.
- [26] The TTF units in both [2]rotaxanes are readily oxidized in the presence of acid. Thus, a dilute buffer ( $5 \times 10^{-4}$  M  $\text{Na}_2\text{CO}_3/\text{NaHCO}_3$ , pH=10) was employed in the subphase of the Langmuir trough.  $\text{CHCl}_3$ , the spreading solvent, was stored over basic alumina and distilled immediately prior to use to keep it free from HCl. The [2]rotaxanes were dissolved in this freshly distilled  $\text{CHCl}_3$  and spread onto the surface of the buffered subphase inside a minute. These precautions were critical for obtaining reproducible and reliable device performance.
- [27] J. H. Schön, H. Meng, Z. Bao, *Nature* **2001**, *413*, 713–716.

Received: April 11, 2002 [F401]